Acta Crystallographica Section D
Biological Crystallography
ISSN 0907-4449

Structural insight into nucleotide recognition in tau-protein kinase I/glycogen synthase kinase 3β

Masaaki Aoki,[a]‡ Takehiro Yokota,[b,c]‡ Ikuko Sugiura,[b,c] Chizuko Sasaki,[b] Tsukasa Hasegawa,[b,c] Chieko Okumura,[b,c] Koichi Ishiguro,[a] Toshiyuki Kohno,[a]* Shigetoshi Sugio[b,c]* and Takao Matsuzaki[b,c]

[a]Mitsubishi Kagaku Institute of Life Sciences (MITILS), 11 Minamiohya, Machida, Tokyo 194-8511, Japan, [b]Mitsubishi Chemical Corporation, Science and Technology Research Center (currently known as Mitsubishi Chemical Corporation, Science and Technology Office, Yokohama Center), 1000 Kamoshida, Aoba, Yokohama 227-8502, Japan, and [c]ZOEGENE Corporation, Research and Development Center, 1000 Kamoshida, Aoba, Yokohama 227-8502, Japan

‡ These authors contributed equally to this work.

Correspondence e-mail: tkohno@libra.ls.m-kagaku.co.jp, ssugio@rc.m-kagaku.co.jp

Received 11 July 2003
Accepted 19 December 2003

PDB References: GSK3β–ADP, 1j1c, r1j1csf; GSK3β–AMPPNP, 1j1b, r1j1bsf.

Human tau-protein kinase I (TPK I; also known as glycogen synthase kinase 3β; GSK3β) is a serine/threonine protein kinase that participates in Alzheimer's disease. Here, binary complex structures of full-length TPK I/GSK3β with the ATP analogues ADP and AMPPNP solved by the X-ray diffraction method at 2.1 and 1.8 Å resolution, respectively, are reported. TPK I/GSK3β is composed of three domains: an N-terminal domain consisting of a closed β-barrel structure, a C-terminal domain containing a 'kinase fold' structure and a small extra-domain subsequent to the C-terminal domain. The catalytic site is between the two major domains and has an ATP-analogue molecule in its ATP-binding site. The adenine ring is buried in the hydrophobic pocket and interacts specifically with the main-chain atoms of the hinge loop. The overall structure and substrate-binding residues are similar to those observed in other Ser/Thr protein kinases, while Arg141 (which is not conserved among other Ser/Thr protein kinases) is one of the key residues for specific ATP/ADP recognition by TPK I/GSK3β. No residues are phosphorylated, while the orientation of the activation loop in TPK I/GSK3β is similar to that in phosphorylated CDK2 and ERK2, suggesting that TPK I/GSK3β falls into a conformation that enables it to be constitutively active.

1. Introduction

The histopathological changes of Alzheimer's disease (AD) are characterized by pathological extracellular deposits of amyloid-β (Aβ) protein in the core of senile plaques, intracellular neurofibrillary tangles (NFT) and extensive neuronal cell loss (Kidd, 1963; Yankner *et al.*, 1990). The main components of NFT are paired helical filaments (PHF), which are composed predominantly of excessively phosphorylated tau protein (Grundke-Iqbal, Iqbal, Quinlan *et al.*, 1986; Grundke-Iqbal, Iqbal, Tung *et al.*, 1986; Wang *et al.*, 1996*a*). Tau proteins are a group of microtubule-associated proteins found in high abundance in neurons of the mammalian brain that promote microtubule polymerization and stabilization and also cross-link axonal microtubules with other cytoskeletal elements such as neurofilaments. Thereby, tau protein supports functions in intracellular trafficking, including axonal transport. The highly phosphorylated tau proteins found in PHF are not only microtubule-assembly incompetent (Iqbal *et al.*, 1994; Wang *et al.*, 1995, 1996*b*), but also inhibit the assembly of microtubules and disassemble the reassembled microtubules *in vitro* (Alonso *et al.*, 1994, 1996, 1997).

Many protein kinases have been examined for their relative contributions to the phosphorylation state of tau protein and to neuronal signal transduction pathways thought to be altered in AD. Although a number of protein kinases can

phosphorylate tau protein *in vitro*, the most physiologically relevant appears to be tau-protein kinase I (Ishiguro *et al.*, 1992). Human tau-protein kinase I (TPK I; EC 2.7.1.135) is a serine/threonine proline-directed kinase purified from the microtubule fraction of brain tissue and its amino-acid sequence is identical to that of glycogen synthase kinase 3β (GSK3β; EC 2.7.1.37; Ishiguro *et al.*, 1993). Although this enzyme is neurochemically known as TPK I, we will refer to it in this paper by the internationally and biochemically accepted name GSK3β. GSK3β creates PHF epitopes on tau protein and the sites of phophorylation by GSK3β in tau protein account for those commonly found in PHF (Imahori & Uchida, 1997). GSK3β has an unique recognition of substrate protein/peptides compared with other kinases. It is one of the few kinases that prefer prior phosphorylation of the substrate before further phosphorylating it. It should be noted that the activity of GSK3β is regulated by neuronal signalling pathways stimulated by Aβ protein. Treatment of rat hippocampus cultures with Aβ protein causes neuronal cell death and stimulates tau-protein phosphorylation in a PHF-like manner. Pretreatment of the cells with antisense oligonucleotides for GSK3β prevented Aβ toxicity, indicating GSK3β to be one of the protein kinases responsive to the stimulus (Takashima *et al.*, 1993). Furthermore, the Aβ stimulus activated GSK3β and inactivated phosphatidylinositol 3-kinase, which is proposed to be a regulator of GSK3β activity. The findings indicate that GSK3β plays a central role in the hypothesis of neuronal cell death induced by Aβ and that GSK3β is one of the potential targets for inhibitor drugs against AD.

The three-dimensional structure of GSK3β has recently been determined and its substrate peptide/protein-recognition and phosphorylation mechanisms have been analyzed (Dajani *et al.*, 2001; Haar *et al.*, 2001; Bax *et al.*, 2001); there is no structural knowledge regarding the recognition of ATP, as these crystal structures were free of ATP analogues. In this paper, we report the first binary complex structures of GSK3β with the ATP analogues ADP and AMPPNP in order to provide structural insights into nucleotide recognition in GSK3β.

2. Materials and methods

2.1. Enzyme preparation

Full-length human GSK3β was expressed in *Escherichia coli* as a fusion protein with a Leu-Glu-His_6 tag at the C-terminus (428 amino-acid residues) and was purified as described previously (Aoki *et al.*, 2000). The N-terminal sequence used in this work was determined by Edman degradation and revealed that the N-terminal methionine residue (Met1) was removed post-translationally in the *E. coli* host. No phosphorylation was detected within the protein, as judged by LC-MS/MS analysis of its protease digests and GelCode Phosphoprotein Staining Kit (Pierce Chemical Co.). Purified GSK3β showed a single band on SDS–PAGE and was concentrated to 10 mg ml^{-1} with 2 m*M* ATP or AMPPNP. The protein concentration was determined using a Non-Interfering Protein Assay Kit (Geno Technology Inc.) using bovine serum albumin as a standard.

Table 1
Data-collection statistics.

	GSK3β–ADP		GSK3β–AMPPNP	
	Native-1	Native-2†	EMTS	Native-3
X-ray source	PF	SPring-8	SPring-8	SPring-8
Beamline	BL6A	BL24XU	BL24XU	BL24XU
Detector	Quantum 4R	R-AXIS IV	R-AXIS IV	R-AXIS IV
Wavelength (Å)	1.000	0.835	0.835	0.835
Resolution (Å)	44.7–2.3	20.0–2.0	31.6–2.6	19.8–1.7
No. observations	550969	619714	283718	525854
No. unique reflections	56967	86325	39715	115006
Completeness (%)	99.7	99.4	99.5	90.0
Redundancy	9.6	7.2	7.1	6.4
$\langle I\rangle$/SD	17.7	18.3	27.0	18.4
R_{merge} (%)	10.9	7.0	6.4	5.6
Space group	$P2_12_12_1$	$P2_12_12_1$	$P2_12_12_1$	$P2_12_12_1$
Unit-cell parameters (Å)				
a	82.9	82.9	82.9	82.8
b	86.1	86.1	86.1	86.3
c	178.1	178.1	178.1	178.4

† The Native-2 data set was used for structural refinement.

2.2. Crystallization and data collection

Purified GSK3β–ATP and GSK3β–AMPPNP were co-crystallized with solutions containing 12–14%(*w*/*v*) PEG 6000, 100 m*M* NaCl, 5 m*M* $MgCl_2$, 10%(*v*/*v*) glycerol in 100 m*M* HEPES–NaOH buffer pH 7.5 by hanging-drop vapour diffusion at 278 K (Aoki *et al.*, 2000) and crystals were grown within several days to maximum dimensions of 0.5 × 0.4 × 0.3 mm. A heavy-atom derivative was prepared by soaking a native crystal in crystallization solution containing 0.1 m*M* ethylmercuric thiosalicylate (EMTS) at pH 7.5 for 1 h. Crystals were transferred to a crystallization solution containing 30%(*w*/*v*) D-sorbitol as a cryoprotectant and were flash-cooled in a nitrogen-gas stream at 100 K.

X-ray diffraction data were collected using synchrotron radiation at BL6A, Photon Factory (KEK, Japan) with a Quantum 4 CCD detector (Area Detector Systems Co.) and BL24XU, SPring-8 with an R-AXIS IV imaging-plate detector (Rigaku Co.). Intensity data were indexed, integrated and scaled using the program *MOSFLM* (Leslie, 1998). Subsequent data processing was performed with the *CCP*4 program suite (Collaborative Computational Project, Number 4, 1994). The crystals belong to the orthorhombic space group $P2_12_12_1$, with unit-cell parameters a = 82.9, b = 86.1, c = 178.1 Å. The asymmetric unit contains two molecules of GSK3β (MW = 48 kDa), giving a Matthews constant (Matthews, 1968) of 3.3 $Å^3$ Da^{-1}. Intensity statistics are summarized in Table 1.

2.3. Structure modelling and refinement

For the GSK3β–ADP complex, the initial phase was solved by single isomorphous replacement including anomalous scattering from an EMTS derivative at 3.0 Å resolution. Eight Hg sites were found both in isomorphous and anomalous difference Patterson maps. There are two protein molecules in

the asymmetric unit and four Hg sites (Cys76, Cys107, Cys199 and Cys317) in each molecule. Phase information was extended to 2.7 Å resolution with solvent flattening and NCS averaging using the *CCP*4 program suite. After constructing the initial atomic model, another native data set was obtained at 2.1 Å resolution, which was then used for the remaining structural refinement. The atomic model was refined with the program *X-PLOR*98.1 (Brünger *et al.*, 1998) and model building and fitting were performed with the program *XtalView* (McRee, 1993). The final structure refined at 2.1 Å resolution gave a crystallographic *R* factor and a free *R* factor of 0.22 and 0.24, respectively. The r.m.s.d.s from the ideal values were 0.007 Å for bond lengths and 1.173° for bond angles, and the average *B* factors were 1.163 Å^2 for bonds and 2.004 Å^2 for angles (Table 2). Refinement statistics are summarized in Table 2. There are two GSK3β molecules (molecules *A* and *B*) in the asymmetric unit, together with 267 water molecules, two ADP molecules and two magnesium ions in the final atomic coordinates. Although GSK3β was co-crystallized with ATP, only an ADP moiety was found in the density map (Fig. 1*a*), suggesting that most ATP molecules in the crystal were hydrolyzed during crystal growth.

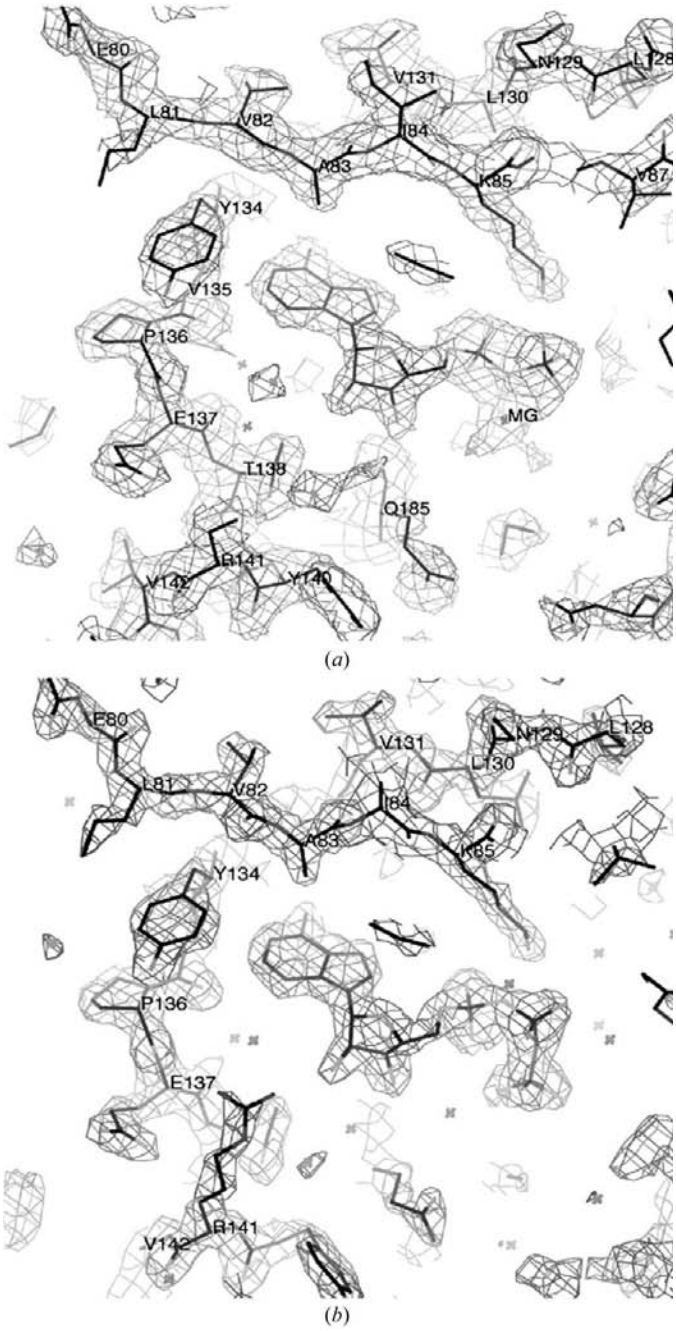

Figure 1
Electron-density maps of (*a*) the ADP molecule and (*b*) the AMPPNP molecule bound in the ATP-binding site of GSK3β. Electron density is calculated with $2F_{obs} - F_{calc}$ coefficients and is drawn at the 1.5σ level. These figures were produced using the program *XtalView*.

Table 2
Structure-refinement statistics.

Values in parentheses refer to the last resolution shell.

	GSK3β–ADP	GSK3β–AMPPNP
Resolution (Å)	15.0–2.1 (2.15–2.10)	20.0–1.8 (1.84–1.80)
No. reflections	74557 (4670)	110728 (6175)
Completeness (%)	94.6 (95.0)	88.6 (79.2)
R factor (%)	21.8 (27.8)	21.6 (28.6)
R_{free} (%)	24.2 (33.4)	24.2 (31.8)
No. of atoms (2 molecules)	6062	6220
GSK3β	5739	5739
Ions (Mg^{2+})	2	0
Waters	267	419
R.m.s. deviations		
Distances (Å)	0.007	0.007
Angles (°)	1.17	1.15
Improper angles (°)	0.65	0.65
Dihedral angles (°)	24.7	24.6
Ramachandran statistics (No. of non-Gly and non-Pro residues in molecules *A* and *B*)		
Most favoured regions	269/308 and 266/316	263/308 and 369/316
Additional allowed regions	35/308 and 46/316	42/308 and 44/316
Generously allowed regions	2/308 and 2/316	1/308 and 1/316
Disallowed regions	2/308 and 2/316	2/308 and 2/316

For the GSK3β–AMPPNP complex, the initial phase at 1.8 Å resolution (Native-3) was determined by molecular replacement using the structure of the GSK3β–ADP complex at 2.1 Å resolution (Native-2) as a probe model. The model was refined with *X-PLOR*98.1 and model building and fitting were performed with *XtalView*. The final structure gave a crystallographic *R* factor and a free *R* factor of 0.22 and 0.24, respectively. The r.m.s.d.s from the ideal values are 0.007 Å for bond lengths and 1.148° for bond angles and the average *B* factors are 1.183 Å^2 for bonds and 2.037 Å^2 for angles. Refinement statistics are summarized in Table 2. There are two GSK3β molecules in the asymmetric unit, together with 419 water molecules and two AMPPNP molecules. Electron density for AMPPNP was clearly found in the active site, while that for magnesium ion was not detected (Fig. 1*b*).

In both complex structures, the Ramachandran plot indicates that the backbone torsion angles for most non-glycine residues fall within the favourable and the acceptable regions, with the exception of Lys123, Cys218, Tyr221 and Asn370. The atomic positions of these four residues are unambiguously defined by distinct electron density, although their backbone conformation seems to be energetically unfavourable. The side chains of Arg220 in both molecules *A* and *B* sit very close

to the non-crystallographic twofold axis and electron density for their guanidyl group is completely missing. Electron density for Ser2–Gly34 and Ser389–His428 in molecule *A*, and Ser2–Ala22 and Ala387–His428 in molecule *B* are not visible, presumably owing to structural disorder, and these regions (N- and C-termini) were not assigned in the final atomic model.

3. Results and discussion

3.1. Overall structures

GSK3β forms a dimeric quaternary assembly in all known crystal structures, in which two molecules (molecules *A* and *B*) in the asymmetric unit are related to each other by non-crystallographic twofold symmetry (Dajani *et al.*, 2001; Haar *et al.*, 2001; Bax *et al.*, 2001). The active centre of each protein molecule exists independently and has one molecule of ATP analogue in the ATP-binding site. The r.m.s. differences for main-chain atoms between the two molecules in the GSK3β–ADP and GSK3β–AMPPNP complexes are 0.46 and 0.44 Å, respectively. The structural deviations occur at the turns between β-strands, *i.e.* Gln46–Pro51, Cys76–Glu80 and Lys91–Phe93, probably owing to structural flexibility in these regions. GSK3β is composed of three domains: an N-terminal domain (residues 23–133), containing a incomplete β-barrel structure with seven antiparallel β-strands, an α-helical C-terminal domain (residues 137–343) and a small extra-domain (residues 344–388) subsequent to the C-terminal domain (Fig. 2). Electron density corresponding to the N- and C-terminal regions of GSK3β is not visible; these regions are thought to be very flexible.

Compared with the structural variations between the two molecules in the same crystal structure mentioned above, the

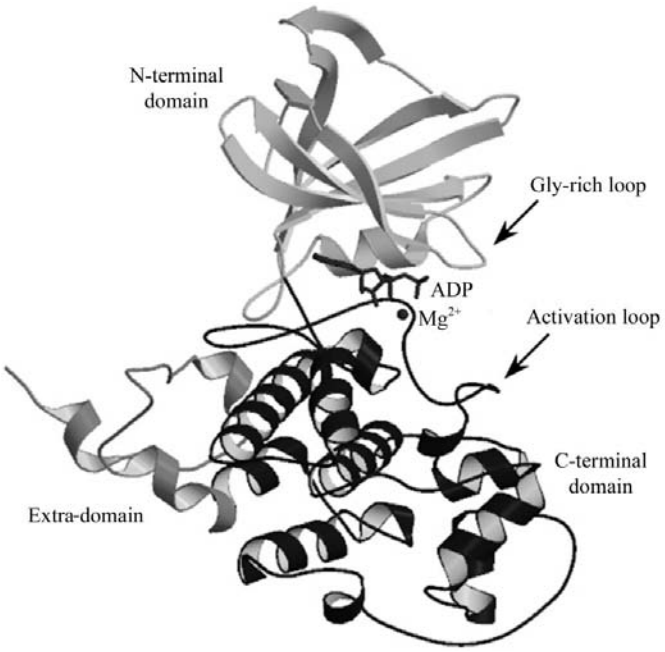

Figure 2
Overall structure of GSK3β complexed with an ATP analogue (molecule *B* of the GSK3β–ADP complex is shown as an example). GSK3β is drawn as a ribbon model (helices and strands represented as coils and arrows) and the three domains are shown in light grey (N-terminal), black (C-terminal) and dark grey (extra). The ADP molecule and magnesium ion bound between the N- and C-terminal domains are shown in black in stick representation and as a sphere, respectively. This figure was produced using the program *MOLSCRIPT* (Kraulis, 1991).

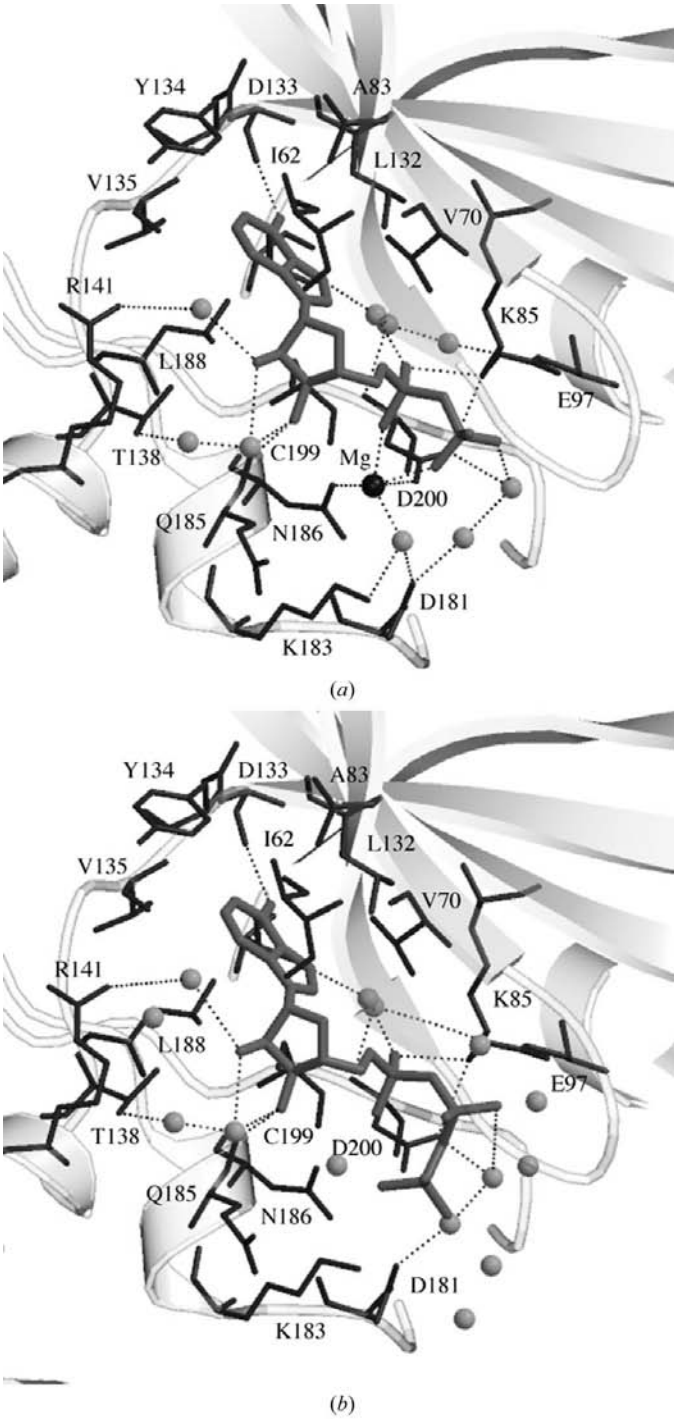

Figure 3
Residues participating in binding of (*a*) ADP and (*b*) AMPPNP in the ATP-binding site of GSK3β. GSK3β is drawn as a white ribbon; amino-acid residues, ATP analogues, magnesium ion and water molecules are shown as black sticks, grey sticks, a black sphere and light grey spheres, respectively. Hydrogen bonds are shown as dotted lines. These figures were produced using the program *MOLSCRIPT*.

r.m.s. deviations for all main-chain atoms between different crystal structures are surprisingly small, *i.e.* 0.67 Å between uncomplexed GSK3β (PDB code 1i09; Haar *et al.*, 2001) and the ADP complex, and 0.68 Å between uncomplexed GSK3β and the AMPPNP complex. Therefore, the overall structure of GSK3β is little affected by complex formation with ATP analogues.

3.2. ATP-binding site

The ADP molecule binds to the amino-acid residues in the cleft between the two main domains (Fig. 2). The nucleotide bound in the complex adopts the *anti* conformation, the same as most ADP/ATP molecules bound to protein kinases. The adenine ring is buried in the hydrophobic pocket formed by Ile62, Val70, Ala83, Val110, Leu132 and Leu188. The purine base also interacts specifically with the main-chain atoms of a hinge loop connecting the N- and C-terminal domains; namely, the N6 atom interacts with Asp133 O (Fig. 3*a*). A connection between Arg141 NH2 and the N3 atom of the adenine ring *via* two water molecules is found in molecule *A*, but the side chain of Arg141 in molecule *B* is away from the ring and is exposed to the surface. Arg141 NH1 in molecule *B* makes a hydrogen bond with the carbonyl O atom of Pro136, which is at the end of the hinge loop, resulting in a rigid conformation of the hinge. The hydrogen-bonding network plays an important role in fitting the adenine ring to the hinge loop. Arg141 NH2 (in molecule *A*) also interacts through water molecules with the O2′ atom of the sugar. Arg141 is not conserved among protein kinases; the corresponding residue of cAMP-dependent protein kinase is Ser130 and water molecules occupy the space corresponding to Arg141. The O3′ atom of the sugar makes hydrogen bonds to the main-chain carboxyl O atom of Gln185 and the hydroxyl O atom of Thr138 *via* two water molecules. The side chain of Lys85 that interacts with the α- and β-phosphoryl groups is conserved among protein kinases and assists in stabilizing the phosphoryl group during phosphorylation. The consensus sequence Gly-Xaa-Gly-Xaa-Xaa-Gly (the 'glycine-rich motif'; Bossemeyer, 1994) of protein kinases is also found in GSK3β. This motif forms a large anion hole with seven consecutive main-chain amide groups and interacts with the α- and β-phosphates of ADP either directly or through water molecules. In some protein kinases the positive terminus of an α-helix in the N-terminal domain points towards the β- or γ-phosphate of ATP; the helix dipole thus electrostatically stabilizes the phosphoryl group during phosphorylation. However, the N-terminus of the α-helix in GSK3β–ADP is distant from the phosphoryl groups of the nucleotide. The binding orientation of the AMPPNP molecule at the nucleotide-binding site of GSK3β is similar to that in the ADP complex and the residues corresponding to ADP binding are completely conserved in AMPPNP binding (Fig. 3*b*).

The structural distinction between ADP and AMPPNP is only the presence of the γ-phosphoryl group. The α- and β-phosphoryl O atoms (O1G and O2G) do not interact with GSK3β, while the γ-phosphoryl O atom (O3G) forms a hydrogen bond with the OD1 atom of Asn186 in the AMPPNP complex.

3.3. Magnesium-binding site

The magnesium-binding site lies between the two main domains. Spherical electron density is unambiguously assigned

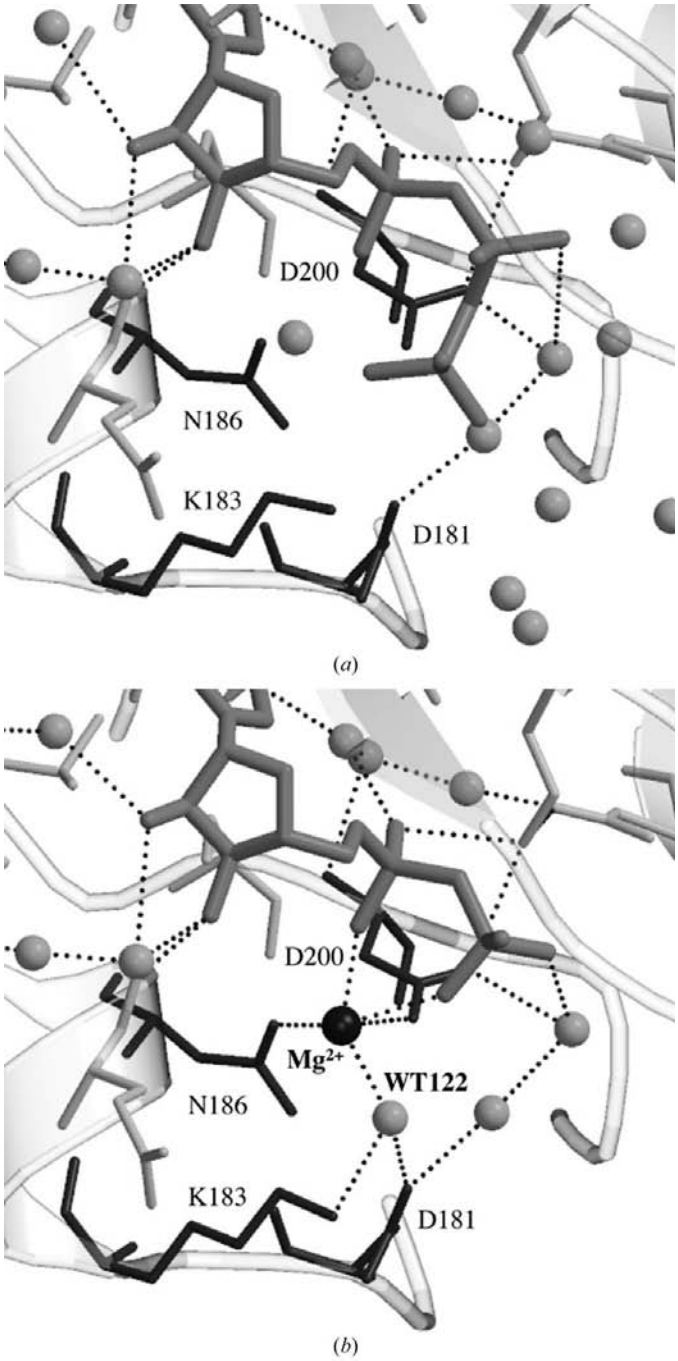

Figure 4
Magnesium-binding site in (*a*) the GSK3β–ADP complex and (*b*) the GSK3β–AMPPNP complex. GSK3β is drawn as a white ribbon; amino-acid residues, ATP analogues, magnesium ion and water molecules are shown as black sticks, grey sticks, a black sphere and light grey spheres, respectively. Hydrogen bonds are shown as dotted lines. These figures were produced using the program *MOLSCRIPT*.

to a magnesium ion in the GSK3β–ADP complex (Fig. 1*a*), while there is no magnesium ion in the GSK3β–AMPPNP complex (Fig. 1*b*). The magnesium ion, which coordinates to the α- and β-phosphoryl O atoms, creates the correct geometry for phosphoryl transfer. The magnesium ion has octahedral coordination with six O atoms from α- and β-phosphoryl groups, asparagine, aspartate and two water molecules in other protein kinases. In the GSK3β–ADP complex, the two water molecules coordinated to the magnesium ion are not found in molecule *A* and only one water molecule is found in molecule *B*; therefore, the magnesium ion is coordinated by only five O atoms from the α- and β-phosphoryl O atoms (O2A and O1B), Asn186 OD1, Asp200 OD2 and one water molecule (WT122) (Fig. 4*a*).

Why is there no magnesium ion in the GSK3β-AMPPNP complex? The magnesium-binding residues are completely conserved in both structures, while one water molecule (WT122) that makes a hydrogen bond with magnesium ion in the ADP complex is missing in the AMPPNP complex. The γ-phosphoryl group of AMPPNP occupies a similar position as the magnesium ion in the GSK3β–ADP complex (0.51 Å from O3G to the magnesium ion). As a consequence, there is no space for either the magnesium ion or the water molecule to occupy in the AMPPNP complex. The binding mode of phosphoryl groups in the AMPPNP complex therefore seems to be unproductive in terms of phosphorylation.

3.4. Activation-loop structure

The catalytic activity of Ser/Thr protein kinases primarily depends upon the correct juxtaposition of the catalytic groups contributing to the transfer of the γ-phosphate group from an ATP molecule to a serine or threonine residue of the protein substrate. The activity secondarily depends on the accessibility and the correct positioning of the groups forming the substrate-binding site, which provide affinity and specificity for the substrate (Johnson *et al.*, 1996). In many protein kinases, these two requirements are simultaneously contingent

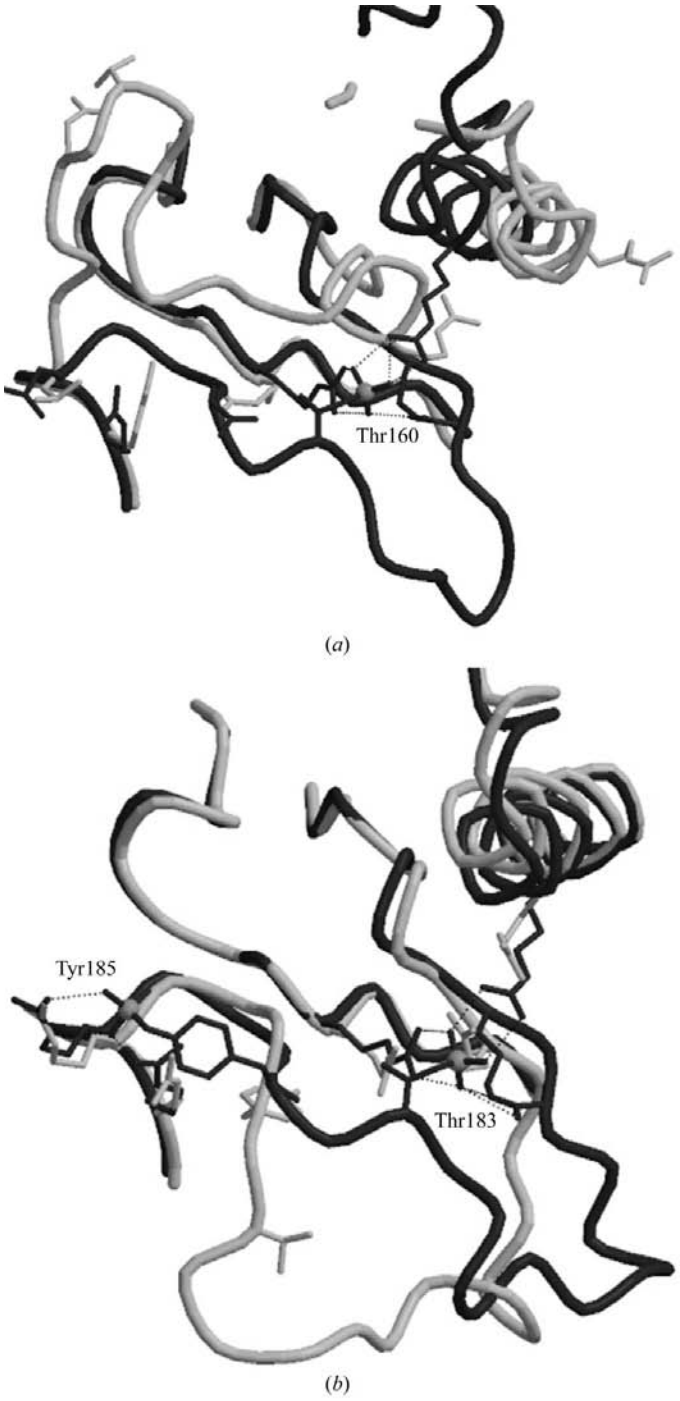

Figure 5
Conformational changes of the activation loop in unphosphorylated/phosphorylated protein kinases: (*a*) CDK2, (*b*) ERK2. The loops are drawn as tubes and unphosphorylated and phosphorylated proteins are shown in light grey and black, respectively. (*c*) Structural comparison between phosphorylated CDK2 (dark grey), phosphorylated ERK2 (light grey) and unphosphorylated GSK3β (black). These figures were produced using the program *MOLSCRIPT*.

upon the conformation of the activation loop containing residues that are themselves subject to phosphorylation.

Comparison of GSK3β with other kinases, such as cyclin-dependent kinase 2 (CDK2) and extracellular-regulated kinase 2 (ERK2), revealed that the conformation of the activation loop in GSK3β closely resembles that in the activated form of protein kinases (Brown *et al.*, 1999; Canagarajah *et al.*, 1997). The activation loop in GSK3β is well ordered and positioned against the α-helical domain. This orientation opens the substrate-binding groove and mimics the position of the activation loop in activated substrate-bound CDK2 and ERK2 (Figs. 5*a* and 5*b*). The conformation of the activation loop in GSK3β is similar to that in phosphorylated CDK2 and ERK2 (Fig. 5c). The side chain of Thr160 in CDK2 and those of Thr183 and Tyr185 in ERK2 are phosphorylated in their active conformation, while that of Tyr216 in GSK3β is not. It is noteworthy that there is no threonine residue in the activation loop of GSK3β to be phosphorylated upon activation; the corresponding residue to Thr160 in CDK2 and Thr183 in ERK2 is Val214 in GSK3β. Although Dajani *et al.* (2001) and Haar *et al.* (2001) have recently reported that anions bind to the activation loop, no anions were found in our GSK3β–ATP analogue complexes. Thus, the activation loop in GSK3β always forms an activated/open conformation without phosphorylation.

3.5. Substrate-binding site

In the phosphorylation mechanism of substrate protein/peptide by protein kinases, GSK3β has a unique choice of substrates compared with other kinases. GSK3β is one of the few kinases that prefer substrate that is phosphorylated prior to the phosphorylation by the kinase itself; the consensus sequence of preferable substrate for GSK3β has previously been shown to be Ser/Thr-Xaa-Xaa-Xaa-pSer/pThr (Ishiguro *et al.*, 1992). The substrate-binding site lies between the glycine-rich loop and the activation loop and contains basic residues such as Arg96, Arg180, Lys205, Arg220 and Arg223. The primed phosphorylation residue on the consensus sequence of substrate is firstly recognized and captured at the 'P + 4' site by the positively charged residues Arg96, Arg180 and Lys205. Although these residues are conserved in other Ser/Thr protein kinases, such as Arg50, Arg126 and Arg150 in CDK2 and Arg68, Arg146 and Arg170 in ERK2, they play a totally different role, *i.e.* tethering the phosphorylated threonine on the activation loop, and do not participate in substrate recognition. As GSK3β does not have such a threonine on its activation loop, these positively charged residues wholly contribute to the unique substrate specificity in GSK3β (Fig. 6). The γ-phosphoryl group of ATP is then transferred to the serine or threonine residue to be phosphorylated by the catalytic residues Lys85, Glu97, Asp181 and Asp200, which are completely conserved in CDK2 (Lys33, Glu51, Asp127 and Asp145) and ERK2 (Lys52, Glu69, Asp147 and Asp165) at the 'P + 0' site.

A patent on the crystal structures (atomic coordinates) of TPK I/GSK3β with ATP analogues was taken out on 5 November 2002 (P2002-320474) at Japan Patent Office.

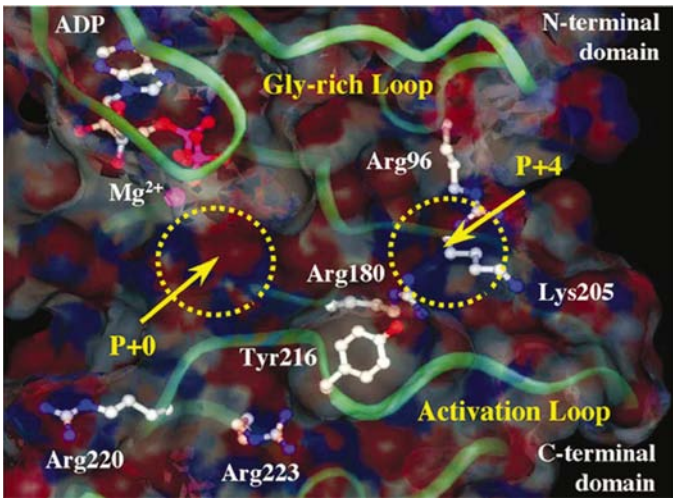

Figure 6
ATP-binding site, magnesium-binding site and substrate-binding site in the GSK3β–ADP complex. GSK3β is drawn as green tubes and a partially transparent surface on which electrostatic potential is mapped as red (negative) and blue (positive). Amino-acid residues and the ADP molecule are shown in ball-and-stick representation and the magnesium ion is shown as a magenta sphere. Yellow dotted circles represent substrate-binding pockets in which the P + 0 and P + 4 residues of peptide substrate are charged. This figures was produced using the program *MOLSCRIPT*.

We are grateful to Drs Akihiko Takashima and Showbu Sato for their gift of cDNA encoding human TPK I/GSK3β, Miss Rika Kato and Dr Akira Omori for N-terminal sequence analysis and Mr Mamoru Satoh, Drs Yoshio Kodera and Tadakazu Maeda for post-translational modification analysis by LC-MS/MS. This research was supported in part by the Sakabe project of Tsukuba Advanced Research Alliance (TARA), University of Tsukuba and by a Grant for the National Project on Protein Structural and Functional Analyses from MEXT (the Japanese Ministry of Education, Culture, Sports, Science, and Technology). The synchrotron-radiation experiments at SPring-8 (proposal No. 1999 B24XU-519N) were performed with the approval of the Japan Synchrotron Radiation Research Institute (JASRI).

References

Alonso, A. C., Grundke-Iqbal, I., Barra, H. S. & Iqbal, K. (1997). *Proc. Natl Acad. Sci. USA*, **94**, 298–303.
Alonso, A. C., Grundke-Iqbal, I. & Iqbal, K. (1996). *Nature Med.* **2**, 783–787.
Alonso, A. C., Zaidi, T., Grundke-Iqbal, I. & Iqbal, K. (1994). *Proc. Natl Acad. Sci. USA*, **91**, 5562–5566.
Aoki, M., Iwamoto-Sugai, M., Sugiura, I., Sasaki, C., Hasegawa, T., Okumura, C., Sugio, S., Kohno, T. & Matsuzaki, T. (2000). *Acta Cryst.* D**56**, 1464–1465.
Bax, B., Carter, P. S., Lewis, C., Guy, A. R., Bridges, A., Tanner, R., Pettman, G., Mannix, C., Culbert, A. A., Brown, M. J., Smith, D. G. & Reith, A. D. (2001). *Structure*, **9**, 1143–1152.
Bossemeyer, D. (1994). *Trends Biochem. Sci.* **19**, 201–205.
Brown, N. R., Noble, M. E. M., Endicott, J. A. & Johnson, L. N. (1999). *Nature Cell Biol.* **1**, 438–443.
Brünger, A. T., Adams, P. D., Clore, G. M., DeLano, W. L., Gros, P., Grosse-Kunstleve, R. W., Jiang, J.-S., Kuszewski, J., Nilges, M.,

Pannu, N. S., Read, R. J., Rice, L. M., Simonson, T. & Warren, G. L. (1998). *Acta Cryst.* D**54**, 905–921.
Canagarajah, B. J., Khokhlatchev, A., Cobb, M. H. & Goldsmith, E. J. (1997). *Cell*, **90**, 859–869.
Collaborative Computational Project, Number 4 (1994). *Acta Cryst.* D**50**, 760–763.
Dajani, R., Fraser, E., Roe, S. M., Young, N., Good, V., Dale, T. C. & Pearl, L. H. (2001). *Cell*, **105**, 721–732.
Grundke-Iqbal, I., Iqbal, K., Quinlan, M., Tung, Y.-C., Zaidi, M. S. & Winsniewski, H. M. (1986). *J. Biol. Chem.* **261**, 6084–6089.
Grundke-Iqbal, I., Iqbal, K., Tung, Y.-C., Quinlan, M., Winsniewski, H. M. & Binder, L. I. (1986). *Proc. Natl Acad. Sci. USA*, **83**, 4913–4917.
Haar, E. T., Coll, J. T., Austen, D. A., Hsiao, H. M., Swenson, L. & Jain, J. (2001). *Nature Struct. Biol.* **8**, 593–596.
Imahori, K. & Uchida, T. (1997). *J. Biochem.* **121**, 179–188.
Iqbal, K., Alonso, A. C., Gong, C. X., Khatoon, S., Singh, T. J. & Grundke-Iqbal, I. (1994). *Mol. Neurobiol.* **9**, 119–123.
Ishiguro, K., Shiratsuchi, A., Sato, S., Omori, A., Arioka, M., Kobayashi, S., Uchida, T. & Imahori, K. (1993). *FEBS Lett.* **325**, 167–172.
Ishiguro, K., Takamatsu, M., Tomizawa, K., Omori, A., Takahashi, M., Arioka, M., Uchida, T. & Imahori, K. (1992). *J. Biol. Chem.* **267**, 10897–10901.
Johnson, L. N., Noble, M. E. M. & Owen, D. J. (1996). *Cell*, **85**, 149–158.
Kidd, M. (1963). *Nature (London)*, **197**, 192–193.
Kraulis, P. J. (1991). *J. Appl. Cryst.* **24**, 946–950.
Leslie, A. G. W. (1998). *MOSFLM Users Guide.* MRC Laboratory of Molecular Biology, Cambridge.
McRee, D. E. (1993). *Practical Protein Crystallography.* New York: Academic Press.
Matthews, B. W. (1968). *J. Mol. Biol.* **33**, 491–497.
Takashima, A., Noguchi, K., Sato, K., Hoshino, T. & Imahori, K. (1993). *Proc. Natl Acad. Sci. USA*, **90**, 7789–7793.
Wang, J. Z., Gong, C. X., Zaidi, T., Grundke-Iqbal, I. & Iqbal, K. (1995). *J. Biol. Chem.* **270**, 4854–4860.
Wang, J. Z., Grundke-Iqbal, I. & Iqbal, K. (1996*a*). *Nature Med.* **2**, 871–875.
Wang, J. Z., Grundke-Iqbal, I. & Iqbal, K. (1996*b*). *Brain Res. Mol. Brain Res.* **38**, 200–208.
Yankner, B. A., Duffy, L. K. & Kirschner, D. A. (1990). *Science*, **250**, 279–282.